Optics Letters

Ultra-sensitive slot-waveguide-enhanced Raman spectroscopy for aqueous solutions of non-polar compounds using a functionalized silicon nitride photonic integrated circuit

Zuyang Liu,[1,2,*] Haolan Zhao,[1,2] Bettina Baumgartner,[3] Bernhard Lendl,[3] Andim Stassen,[4] Andre Skirtach,[2,5] Nicolas Le Thomas,[1,2] and Roel Baets[1,2]

[1]*Photonics Research Group, Ghent University-IMEC, 9052 Ghent, Belgium*
[2]*Center for Nano- and Biophotonics, Ghent University, 9052 Ghent, Belgium*
[3]*Institute of Chemical Technologies and Analytics, Technische Universität Wien, 1060 Vienna, Austria*
[4]*IMEC, Kapeldreef 75, 3001 Leuven, Belgium*
[5]*Department of Biotechnology, Ghent University, 9000 Ghent, Belgium*
Corresponding author: zuyang.liu@ugent.be

We demonstrate an ultra-sensitive waveguide-enhanced Raman sensor for low concentration organic compounds dissolved in water. The spectra are obtained using silicon nitride slot waveguides coated with a thin film of hexamethyldisilazane-modified mesoporous silica. Enriched locally by 600-fold within the coating, a micromolar level of cyclohexanone is probed. The sensor is also capable of simultaneous quantification of multiple analytes, and the adsorbed analytes can be completely released from the coating. These properties make this on-chip Raman sensor promising for diverse applications, especially for the monitoring of non-polar organics and biomolecules in aqueous environments. © 2021 Optical Society of America

Raman spectroscopy is a widely acknowledged label-free analytical tool in chemical and biomedical applications [1]. It probes the inelastic scattering of photons by analytes, where the incident light transfers part of its energy to the molecules. Therefore, the scattered light contains the vibrational information of the analytes, which can be used for unambiguous molecular identification and quantification. However, Raman scattering is an extremely weak process. Therefore, the detection limit for low concentration analytes is relatively poor.

Advancements in integrated photonics have opened novel ways to mitigate the limitations associated with the low scattering cross-section of many molecules. Using a single-mode silicon nitride (Si_3N_4) waveguide, the Raman signal of the waveguide cladding can be excited and collected evanescently, a modality called waveguide-enhanced Raman spectroscopy (WERS). A combination of tight mode confinement and enlarged light–matter interaction volume leads to much-enhanced signal intensity, outperforming confocal Raman microscopes [2].

Although WERS has better sensitivity than Raman microscopy, it is still challenging to detect analytes in diluted concentrations with bare Si_3N_4 waveguides. To further improve sensitivity, one method is to enrich the concentration of analytes locally via a sorbent layer. Various sorbents have been adopted to enrich gas-phase chemicals, demonstrating the sensing of warfare agents and volatile organic compounds [3–6]. However, the functionalized waveguides have not been extended to liquid-phase sensing, due mostly to the lack of suitable sorbent materials. For instance, polymer coatings often have poor mechanical stability, as they are prone to swelling [7].

Mesoporous silica is a well-known high-surface-area sorbent [8] that has been used in catalysis [9], separation [10], and sensing [11] due to its versatility in surface chemistry. Functionalized mesoporous silica is promising for liquid-phase WERS for its chemical and mechanical stability. By modifying its surface properties, one can select the adsorbed species and tailor the adsorption characteristics. Recently, mesoporous silica modified by hexamethyldisilazane (HMDS) has been used to enrich benzonitrile and valeronitrile in water [12]. When combined with an HMDS-modified mesoporous silica film, WERS is expected to exhibit excellent sensitivity for non-polar compounds in aqueous solutions, which is common in water quality monitoring [13,14] and the sensing of biomolecules [15,16].

In this work, we demonstrate for the first time ultra-sensitive organic compound Raman sensing in aqueous solutions using a Si_3N_4 slot waveguide top-cladded with an HMDS-modified mesoporous silica layer. We use cyclohexanone and 1-indanone as model analytes. We first introduce the method of fabrication and measurement, then compare the detection limits of WERS sensors with and without the coating. The capability of simultaneous measurement of multiple compounds is also examined.
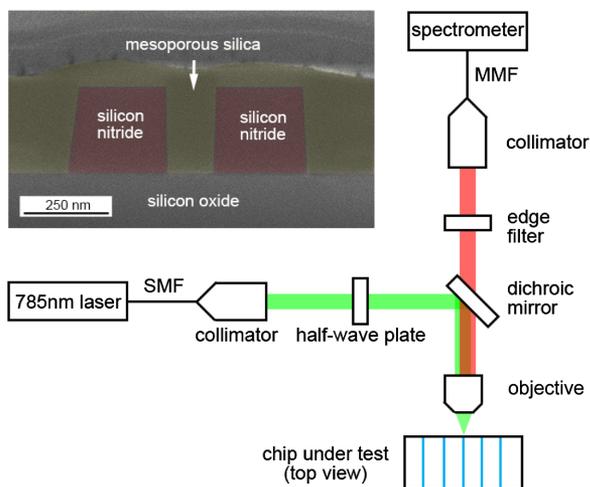
Fig. 1. Experimental setup. Inset: scanning electron micrograph of the cross-section of a Si_3N_4 slot waveguide coated with mesoporous silica.

Finally, we study the desorption behavior with two different solvents: water and isopropyl alcohol (IPA).

The photonic chip is fabricated by IMEC on the BioPIX platform described in [17]. There is a 300-nm-thick Si_3N_4 layer deposited on top of a 2-µm-thick buried oxide via plasma enhanced chemical vapor deposition (PECVD). The slot waveguides are then defined by deep UV lithography and reactive ion etching (RIE), with a gap width of 150 nm and a rail width of 300 nm. The slot waveguides are tapered into 3-µm-wide strip waveguides for edge coupling at both ends. The coupling loss is at most 7.4 dB per facet, which is similar to that in previous experiments using bare Si_3N_4 slot waveguides [18]. A layer of SiO_2 is deposited on top of the Si_3N_4 core as the top cladding. Part of it is later removed to expose a 6-mm-long section for sensing. The waveguides are then coated with a 425-nm-thick layer of mesoporous silica that is later modified with HMDS, as discussed in [12]. The inset of Fig. 1 shows the cross-section of the final waveguide. The effective index of the sorbent is 1.385 when filled with dilute aqueous solutions. With a pump wavelength of 785 nm, the confinement factor of the fundamental quasi-TE mode in the coating is 36%, which is 11% higher than the fundamental quasi-TM mode. It is also 25% higher than the optimal strip waveguide in [19].

The experiment setup is shown in Fig. 1. We use a Toptica XTRA II laser (785 nm) to excite the fundamental quasi-TE mode. The pump power is 60 mW before the objective. The Raman signal is analyzed by a spectrometer equipped with an Andor iDus 401 camera cooled to −60°C. For coupling light in and out of the waveguide, we use an objective with 0.6 NA and 40× magnification. Each spectrum is integrated for 5 s.

The surface of mesoporous silica becomes hydrophobic because of the methyl groups from HMDS. Hence, the adsorbent exhibits a strong affinity to non-polar molecules, and they are expected to enrich hydrophobic molecules from an aqueous solution, leading to a stronger Raman signal and better sensitivity.

Cyclohexanone is a common non-polar solvent in industry. It is employed as a model analyte in our experiments. We dissolve it in IPA with 10%–30% volume concentrations. The result is shown in Fig. 2(a), and we can clearly observe the cyclohexanone
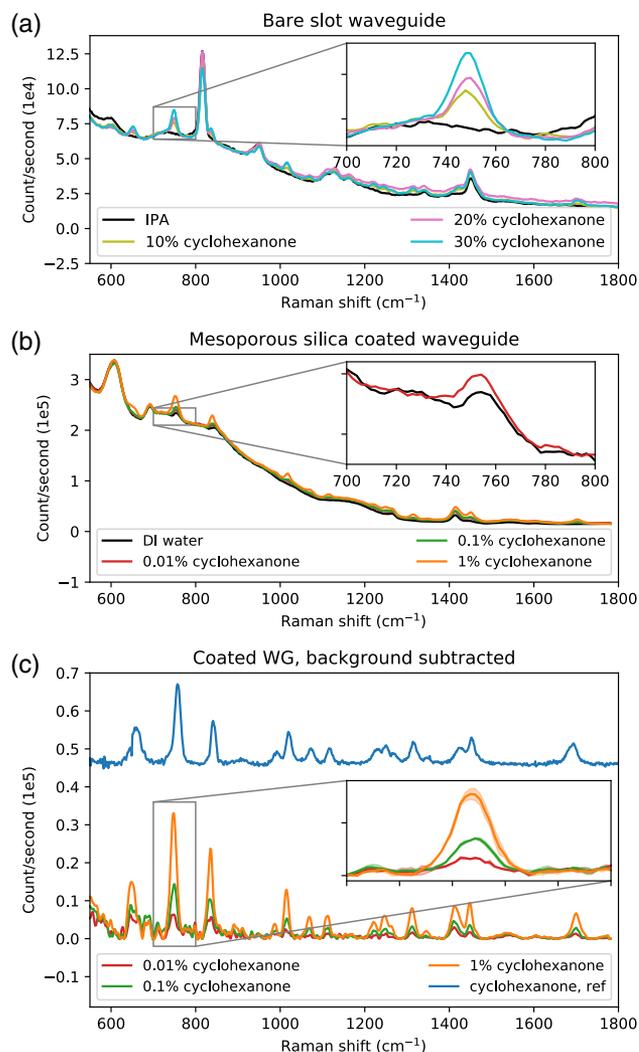

Fig. 2. (a) Raman spectra of IPA and 10%, 20%, and 30% cyclohexanone in IPA on bare Si_3N_4 slot waveguide. (b) Raman spectra of DI water and 0.01%, 0.1%, and 1% cyclohexanone in water on mesoporous silica coated Si_3N_4 slot waveguide. (c) Raman spectra of 0.01%, 0.1%, and 1% cyclohexanone solutions on coated waveguides, without background. The blue curve is a reference spectrum of cyclohexanone. The error bar in the inset corresponds to the deviation over two chips.

peak at 757 cm^{-1}. Its peak height is 8450 count per second (ct/s) with 10% cyclohexanone.

We then move to coated waveguides with cyclohaxanone aqueous solution, and the result is shown in Fig. 2(b). It shows the Raman spectra of deionized (DI) water, 0.01%, 0.1%, and 1% cyclohexanone probed by mesoporous silica coated Si_3N_4 slot waveguides. The chip is cleaned with IPA and DI water between measurements, and the disappearance of cyclohexanone peaks validates the cleanliness of the chip. These spectra are normalized by minimizing the distance between the Raman background around the 757 cm^{-1} peak. We can identify some features induced by the coating in addition to the broad features from the silicon nitride core [20]. The inset of Fig. 2(b) shows the Raman spectra around the 757 cm^{-1} peak with 0.01% cyclohexanone.

To quantify the performance of the coated waveguides, we first subtract the DI water background from the cyclohexanone

results, and then apply baseline correction using the asymmetric least squares method [21]. The results are shown in Fig. 2(c) with the inset zooming onto the 757 cm^{-1} peak. The blue curve is a reference spectrum of pure cyclohexanone measured in bulk liquid using the same confocal Raman microscope. An excellent correspondence can be seen between the reference and the measured spectra. To characterize the reproducibility, cyclohexanone measurements are repeated on another coated waveguide with the same geometry. The deviation between these two measurements is shown as the shaded areas in the inset of Fig. 2(c). The results are highly consistent.

The amount of adsorbed analytes over ambient concentration can typically be characterized by the Langmuir or Freundlich model [22]. On our coated waveguide, with ascending concentration (0.01%–0.1%–1%), the peak height at 757 cm^{-1} increases from 6550, 14,440 to 33080 ct/s, which is consistent with the Freundlich model. Based on this model, the coated waveguide holds the potential to probe analytes in the 10-μm range. In comparison, the peak intensity on the bare slot waveguide varies linearly with analyte concentration. Based on Fig. 2(a), we estimate that 6% cyclohexanone is needed on a bare waveguide to produce the Raman signal of 0.01% cyclohexanone on the coated waveguide. Therefore, at 0.01% cyclohexanone (equal to 970 μm), the enrichment factor of the coating is around 600.

Meanwhile, the peak height of 6550 ct/s for 0.01% cyclohexanone corresponds to a Raman conversion efficiency of 1.65×10^{-12}/cm from pump to Raman signal, with an error margin of 15% by considering the uncertainties in waveguide length, coupling loss, and signal propagation loss within the microscope. In comparison, a conversion efficiency of 10^{-11}/cm for pure IPA is obtained with a Si$_3$N$_4$ strip waveguide [23]. It is equivalent to 7×10^{-16}/cm for 0.01% cyclohexanone, given the difference in molecular density and Raman scattering cross-section. Therefore, the coated slot waveguide outperforms the bare strip waveguide by a factor of around 2200.

The ultimate performance of the coated waveguide can be even higher. However, due to the nonlinear nature of the Freundlich model, an extensive study across multiple samples is necessary to fully quantify the potential of the waveguide sensor.

It is well known that Raman spectroscopy can quantify multiple compounds simultaneously. However, on the coated waveguide, analytes might be competing for limited adsorption sites, and the signal of one compound can be influenced by another.

To characterize the coated waveguides' capability for multiplex sensing, we measure the Raman signal of multiple aqueous solutions comprising varying amounts of cyclohexanone and 1-indanone. 1-Indanone is an aromatic non-polar solid compound that is involved in metabolism and drug synthesis. Figure 3(a) shows the spectrum of 97 mM (1%) cyclohexanone and 7.6 mM (1 g/L) 1-indanone with the DI water background already subtracted. Using the reference spectra obtained from bulk solutions, we can attribute the Raman peaks to each individual analyte, as shown in the inset. It indicates the coated waveguide can at least be used for multiplex identification.

We further investigate the potential for multiplex quantification. Figures 3(b)–3(d) show the Raman spectra of the mixture with different mixing ratios, each measured three consecutive times. Figures 3(b) and 3(c) both have 1.9 mM
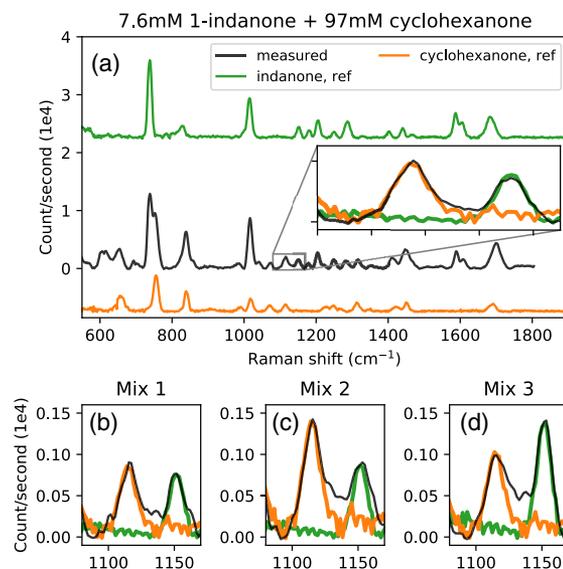
Fig. 3. (a) Background-subtracted spectrum of 7.6 mM (1 g/L) 1-indanone and 97 mM (1%) cyclohexanone solution (black). The orange and green curves show the reference spectra of cyclohexanone and 1-indanone, respectively. The inset shows an enlargement of the range 1075−1175 cm^{-1} and the fitted peak profiles. Raman spectra of the mixture with (b) 1.9 mM (0.25 g/L) 1-indanone and 24 mM (0.25%) cyclohexanone, (c) 1.9 mM 1-indanone and 48 mM (0.5%) cyclohexanone, and (d) 3.8 mM (0.5 g/L) 1-indanone and 24 mM cyclohexanone.

(0.25 g/L) 1-indanone in the solution, while the cyclohexanone concentrations are 24 mM (0.25%) and 48 mM (0.5%), respectively. With twice the amount of cyclohexanone, the peak count of 1-indanone at 1150 cm^{-1} increases slightly from 142 to 167. Similarly, the cyclohexanone signal also slightly increases from 184 to 210 from Figs. 3(c) to 3(d) when the 1-indanone concentration doubles.

We believe this variation in peak height is due to imperfect spectral analysis instead of real physical limitations. In Figs. 3(b)–3(d), the tail of one peak overlaps with the other and leads to a small increase in peak height. The spectrum from individual components can in principle be deconvolved by a well-trained mathematical model. However, building such a model requires a comprehensive mapping of the Raman spectra at varying concentrations, and it is beyond the scope of this study.

Desorption of adsorbed molecules is essential to monitor the variations of the analyte concentration. To examine the desorption properties of the coated waveguide, we first immerse the sample in 45.4 mM 1-indanone aqueous solution until the signal intensity reaches the maximum. Afterward, we quickly remove the solution and apply DI water. Meanwhile, we record the height of the 738 cm^{-1} peak with a 0.1 s integration time.

Figure 4(a) shows the temporal profiles of the signal intensity of two repeated experiments on one sample. The initial plummet of peak count corresponds to the application of DI water, which slightly disturbs the optical alignment between the waveguide and the microscope objective. Then, the peak counts quickly increase as the alignment restores. Also, the application of water reduces the propagation loss, and the peak count even increases beyond its original value. When the desorption reaches an equilibrium ($t > 200$ s), a weak 1-indanone signal is still
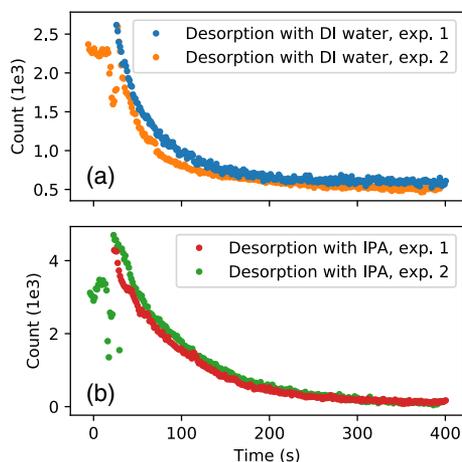
Fig. 4. Desorption profiles of 1-indanone using (a) DI water and (b) IPA. The integration time of each measurement is 0.1 s. Desorption with each solvent was performed two times.

present. It suggests that the applied volume of DI water (approximately 1 mL) cannot fully desorb 1-indanone from the sorbent. However, we would like to emphasize that this is limited by the volume of DI water and the low solubility of 1-indanone in DI water.

To prove the desorption is currently only volume limited, we perform the measurement using IPA instead of DI water on the same chip. As 1-indanone has a higher solubility in IPA, we expect better desorption of indanone from the coating. The results are shown in Fig. 4(b). With the same volume as DI water, IPA almost completely removes the adsorbed 1-indanone.

It is important to note that the signal intensity always restores after immersion in 1-indanone solution again in the desorption tests. This desorption study further indicates the potential of concentration monitoring and the reusability of the coated waveguide.

We present an ultra-sensitive on-chip Raman sensor for the identification and quantification of non-polar molecules in water. Combined with a mesoporous silica coating modified with HMDS, WERS shows much higher signal intensity of cyclohexanone in aqueous solutions compared to bare Si_3N_4 slot waveguides. For the lowest concentration (0.01%, 970 μm) measured on a coated waveguide, the peak count of 6550 ct/s is equivalent to the peak count from 6% cyclohexanone on the bare slot waveguide. It suggests an enrichment factor of 600 in the coating for 0.01% cyclohexanone. The Raman conversion efficiency of 970-μm cyclohexanone solution from pump to Raman signal is 1.65×10^{-12}/cm, with an error margin of 15%, which is three orders of magnitude stronger than bare strip waveguides [23]. We also show unambiguous simultaneous detection of 1-indanone and cyclohexanone. The precision is not significantly affected by the introduction of another compound. Also, DI water with a volume of 1 mL can partly desorb 1-indanone molecules from the sorbent, while 1 mL IPA can virtually remove all the adsorbed molecules within minutes.

It indicates the potential of the coated waveguides for real-time monitoring of hydrophobic analytes.

The combination of Si_3N_4 slot waveguide and HMDS-modified mesoporous silica film is suitable for organic sensing using WERS. With considerable enrichment of non-polar molecules, promising simultaneous detection, and robustness of the sensor, this coated Si_3N_4 waveguide sensor holds potential for diverse applications, including the monitoring of non-polar contaminants and biomolecules in aqueous environments.

REFERENCES

1. J. R. Ferraro, K. Nakamoto, and C. W. Brown, *Introductory Raman Spectroscopy* (Academic, 2003).
2. A. Dhakal, A. Raza, F. Peyskens, A. Z. Subramanian, S. Clemmen, N. Le Thomas, and R. Baets, Opt. Express **23**, 27391 (2015).
3. S. A. Holmstrom, T. H. Stievater, D. A. Kozak, M. W. Pruessner, N. Tyndall, W. S. Rabinovich, R. A. McGill, and J. B. Khurgin, Optica **3**, 891 (2016).
4. N. F. Tyndall, T. H. Stievater, D. A. Kozak, K. Koo, R. A. McGill, M. W. Pruessner, W. S. Rabinovich, and S. A. Holmstrom, Opt. Lett. **43**, 4803 (2018).
5. H. Zhao, B. Baumgartner, A. Raza, A. Skirtach, B. Lendl, and R. Baets, Opt. Lett. **45**, 447 (2020).
6. G. Antonacci, J. Goyvaerts, H. Zhao, B. Baumgartner, B. Lendl, and R. Baets, APL Photon. **5**, 081301 (2020).
7. Y. Lu, L. Han, C. J. Brinker, T. M. Niemczyk, and G. P. Lopez, Sens. Actuators B Chem. **36**, 517 (1996).
8. C. T. Kresge, M. E. Leonowicz, W. J. Roth, J. C. Vartuli, and J. S. Beck, Nature **359**, 710 (1992).
9. J. H. Clark, D. J. Macquarrie, and S. J. Tavener, Dalt. Trans. **0**, 4297 (2006).
10. A. Walcarius and M. M. Collinson, Annu. Rev. Anal. Chem. **2**, 121 (2009).
11. B. J. Melde, B. J. Johnson, and P. T. Charles, Sensors **8**, 5202 (2006).
12. B. Baumgartner, J. Hayden, A. Schwaighofer, and B. Lendl, ACS Appl. Nano Mater. **1**, 7083 (2018).
13. M. Janotta, M. Karlowatz, F. Vogt, and B. Mizaikoff, Anal. Chim. Acta **496**, 339 (2003).
14. A. Walcarius and L. Mercier, J. Mater. Chem. **20**, 4478 (2010).
15. M. Comes, M. Marcos, R. Martínez-Máñez, F. Sancenón, J. Soto, L. Villaescusa, P. Amorós, and D. Beltrán, Adv. Mater. **16**, 1783 (2004).
16. S. Li, X. Jiao, and H. Yang, Langmuir **29**, 1228 (2013).
17. A. Rahim, E. Ryckeboer, A. Z. Subramanian, S. Clemmen, B. Kuyken, A. Dhakal, A. Raza, A. Hermans, M. Muneeb, S. Dhoore, Y. Li, U. Dave, P. Bienstman, N. Le Thomas, G. Roelkens, D. V. Thourhout, P. Helin, S. Severi, X. Rottenberg, and R. Baets, J. Lightwave Technol. **35**, 639 (2017).
18. A. Dhakal, P. C. Wuytens, F. Peyskens, K. Jans, N. Le Thomas, and R. Baets, ACS Photon. **3**, 2141 (2016).
19. A. Raza, S. Clemmen, P. Wuytens, M. De Goede, A. S. K. Tong, N. Le Thomas, C. Liu, J. Suntivich, A. G. Skirtach, S. M. Garcia-Blanco, D. J. Blumenthal, J. S. Wilkinson, and R. Baets, Opt. Express **27**, 23067 (2019).
20. N. Le Thomas, A. Dhakal, A. Raza, F. Peyskens, and R. Baets, Optica **5**, 328 (2018).
21. P. H. C. Eilers, Anal. Chem. **75**, 3631 (2003).
22. K. Y. Foo and B. H. Hameed, Chem. Eng. J. **156**, 2 (2010).
23. A. Dhakal, A. Z. Subramanian, P. Wuytens, F. Peyskens, N. Le Thomas, and R. Baets, Opt. Lett. **39**, 4025 (2014).